BMC Veterinary Research

RESEARCH

Open Access

Genomic sequencing and evolutionary analysis of bovine kobuvirus in Yunnan Province, China

Guojun Wang[1,2†], Qiuhui Deng[1†], Peiying Zhu[2], Veerasak Punyapornwithaya[3], Xuseng Shi[1], Yan Liu[1], Xinhui Duan[1], Zailei Li[1*] and Wengui Li[1*]

Abstract

Background Bovine Kobuvirus (BKV) is an emerging pathogen associated with diarrhea in cattle. Limited reports on its prevalence and genetic characteristics are available. To determine the epidemiology and genetic evolution of BKV strains circulating in Yunnan Province, China, 204 diarrheal samples were collected from cattle farms across five regions for screening for BKV infection.

Results RT-PCR analysis identified 40 BKV-positive samples, yielding an infection rate of 19.6%. Positive samples were inoculated into Vero cells for continuous passage, followed by molecular biology, immunofluorescence, and electron microscopy identification. Two BKV strains, BKV YN-1 2023 and YN-2 2023, were isolated. Whole-genome sequencing revealed genome lengths of 8289 bp and 8291 bp (GenBank No. PV410179 and PV410180), respectively. Phylogenetic analysis demonstrated that both strains belong to genotype B, the dominant genotype circulating in China, and are closely related to the previously reported Chinese strain BKV 13/2021. The genetic similarity of two BKV isolates was analyzed. Genome-wide nucleotide identities ranged from 39.9 to 93.9%, with the highest similarity to BKV13 2021 CHN. ORF analysis showed nucleotide and amino acid similarities of 48.7–93.9% and 29.3–98.5%, respectively. Compared to the BKV13 2021 CHN, both isolates exhibited high conservation in VP0, VP3, and nonstructural proteins (97.8–100%), while the L protein had the lowest similarity (94.7–95.2%). The 5′ UTR showed lower conservation than the 3′ UTR, suggesting regulatory variations.

Conclusions These findings reveal that the circulating BKV strains in Yunnan belong to the globally prevalent genotype B and are widely distributed. This study provides valuable insights into the molecular epidemiology, genetic diversity and evolutionary dynamics of BKV, offering an important reference for developing diagnostics, vaccines and further studies on its pathogenesis.

Keywords Bovine kobuvirus, Genome, Diarrhea, Genetic evolution, Yunnan Province

†Guojun Wang and Qiuhui Deng contributed equally to this work.

*Correspondence:
Zailei Li
lizailei806450449@qq.com
Wengui Li
liwengui@ynau.edu.cn

[1]College of Veterinary Medicine, Yunnan Agricultural University, Kunming 650201, China
[2]Faculty of Veterinary Medicine, Khon Kaen University, Khon Kaen 40002, Thailand
[3]Faculty of Veterinary Medicine, Chiang Mai University, Chiang Mai 50100, Thailand

Background

Bovine kobuvirus (BKV), also known as bovine Aichivirus (AiV), is a member of the genus *Kobuvirus* (KoV) within the family *Picornaviridae*. It is a single-stranded, positive-sense, non-enveloped RNA virus [1]. Based on the phylogenetic analysis of the VP1 gene, Kobuvirus has been classified into six types (A–F), with type D further divided into D1 and D2 [2]. The BKV genome is approximately 8200 to 8300 bp in length and consists of a single open reading frame (ORF) encoding a polyprotein, flanked by a 5′ untranslated region (UTR), a 3′ UTR, and a poly(A) tail. The P1 region, which encodes structural proteins, is proteolytically cleaved into VP0, VP3, and VP1. As the VP1 protein is exposed on the surface of viral particles, it is subject to significant environmental pressures, rendering it the most mutation-prone immunodominant protein in BKV [1, 3, 4]. The viral particle exhibits protrusions on its surface, while receptor-binding sites are located in depressions. The capsid comprises 12 pentamers, each formed by VP0, VP3, and VP1, with no internal capsid proteins [5].

BKV was first identified in 2003 by Japanese researchers in Vero cell cultures contaminated with fetal bovine serum, and the U-1 strain was shown to induce cytopathic effects (CPE) upon serial passage in Vero cells [6]. To date, BKV has been detected in 14 countries, including the United States, Canada, Italy, Egypt, and China, spanning North America, South America, Europe, Asia, and Africa, indicating its widespread geographic distribution [7, 8, 9, 10, 11].

During replication, BKV damages intestinal epithelial cells, particularly the upper third of the villi, causing functional impairment of mature enterocytes. This results in disrupted water reabsorption, compromised immune responses in the gut, and ultimately diarrhea [12].

Diarrhea is a leading cause of mortality in calves, significantly affecting the health and growth of subsequent generations and causing economic losses to the cattle industry. Reports indicate that BKV infection rates in calves range from 4.8 to 38.5%, which has an impact on the cattle industry, posing a growing threat to cattle herds [9, 13]. Moreover, the prevalence of BKV has been increasing in recent years, posing a growing threat to cattle herds.

The objective of this study was to investigate the epidemiological characteristics and genetic evolution of BKV strains circulating in cattle farms in Yunnan Province, China. This study is the first report of BKV in cattle herds in Yunnan Province, China. It provides the epidemiology, clinical symptoms, and pathogenic mechanisms of this virus. Furthermore, the amplification and characterization of the complete genome of circulating BKV strains will contribute to understanding the genetic evolution and molecular epidemiology of this virus, laying the groundwork for future studies on its prevention and control.

Results

Isolation and cultivation

The filtrate from positive samples was inoculated onto Vero cells and subjected to three successive blind passages. Obvious cytopathic effects (CPE) were observed beginning from the fourth passage. From the fourth to the eleventh passage, infected cells exhibited significant CPE, including rounding, shrinkage, detachment, and syncytium formation within 24 to 72 h post-infection (Fig. 1). In contrast, no CPE was observed in the control group.

Detection of BKV infection in Vero cells

RT-PCR

The viral supernatant from the fourth passage, after undergoing three freeze-thaw cycles and centrifugation to remove cellular debris, was collected and subjected to RT-PCR detection to assess the presence of viral RNA. A specific DNA fragment of approximately 631 bp was observed after electrophoresis on a 1% agarose gel (Fig. 2). The PCR product was sequenced by Sangon Biotech and compared with the BKV gene sequences published in GenBank. The sequence similarity ranged from 92.5 to 99%, confirming the successful infection of Vero cells with BKV.

RT-qPCR

The proliferation of BKV in Vero cells was assessed across passages 3, 5, 7, 9, 10, and 11 using the SYBR Green quantitative PCR method. The results demonstrated a steady increase in viral load from passage 3 to passage 11. with passage 11 exhibiting significantly higher titers than passage 3 ($P < 0.0001$) (Fig. 3).

Determination of $TCID_{50}$

Vero cells were seeded in a 96-well cell culture plate. Once the cell density reached approximately 85%, the culture medium was removed, and 100 µL of 10-fold serially diluted BKV viral solution was added. After incubation at 37 °C for 2 h, the viral solution was discarded and replaced with a serum-free cell maintenance medium. The cells were then cultured for 3 to 4 days with daily observations. Using the Reed-Muench method, which estimates the 50% endpoint by calculating the point at which 50% of the wells show a cytopathic effect [14]. The $TCID_{50}$ of the 9th-generation BKV was calculated to be $10^{-6.44}$ /0.1 ml (Table 1).

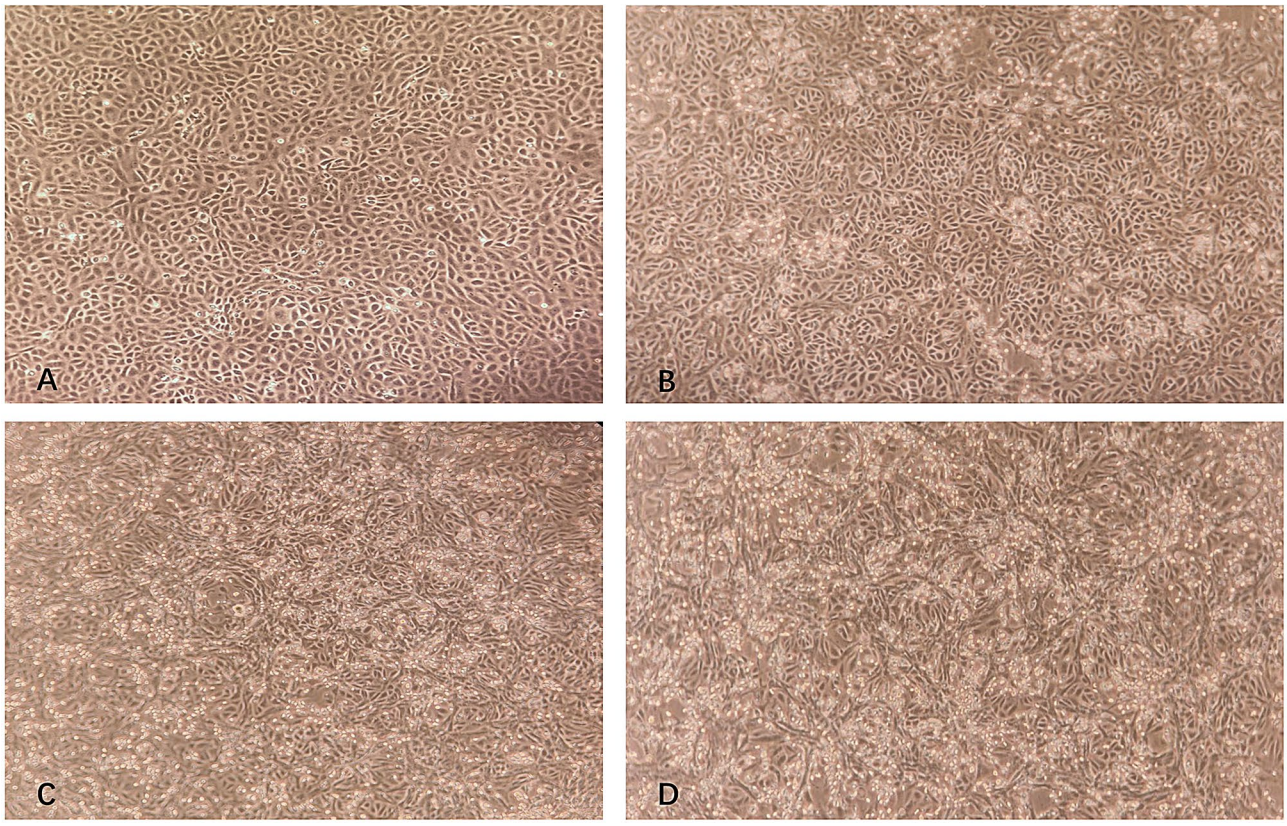

Fig. 1 CPE observed in Vero cells infected with BKV (40× times). **A**: Vero cells uninoculated with the virus; **B**: CPE observed in Vero cells infected by BKV for 24 h; **C**: CPE at 48 h; **D**: CPE at 72 h

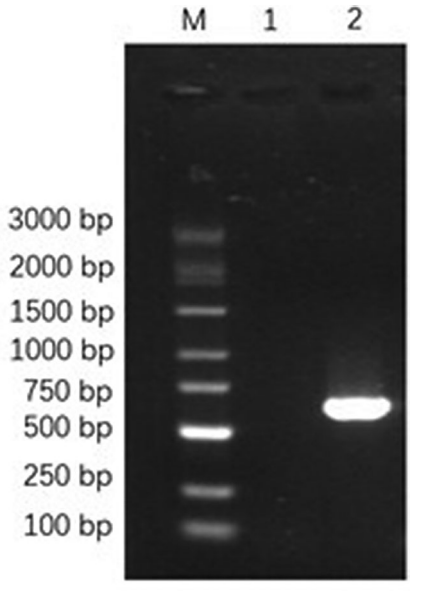

Fig. 2 Results of RT-PCR assay of the 4th generation. M: DL3000Marker; 1:negative control; 2:sample

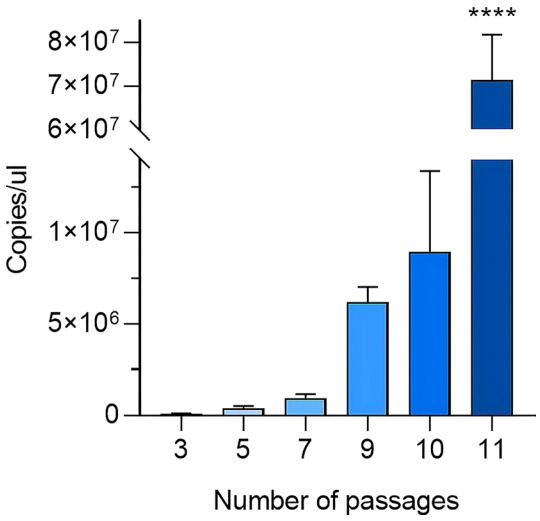

Fig. 3 Changes in the BKV viral load

Immunofluorescence identification

At 48 h post-infection with the viral isolate, the Vero cells were fixed, blocked, and subjected to antigen-antibody binding followed by fluorescent secondary antibody binding. Under an inverted fluorescence microscope, distinct fluorescent signals were observed in the infected cells, indicating the presence of cytopathic effects. The

Table 1 BKV virus induced the number of CPE wells produced in the cells

Virus dilutions	Number of CPE wells	No CPE wells	Grand total		The percentage of CPE holes
			CPE wells number	No CPE wells	
10^{-1}	8	0	51	0	100%(51/51)
10^{-2}	8	0	43	0	100%(43/43)
10^{-3}	8	0	35	0	100%(35/35)
10^{-4}	8	0	27	0	100%(27/27)
10^{-5}	7	1	19	1	95%(19/20)
10^{-6}	5	3	12	4	75%(12/16)
10^{-7}	4	4	7	7	50%(7/14)
10^{-8}	2	6	3	13	18.75%(3/16)
10^{-9}	1	7	1	20	4.76%(1/21)
10^{-10}	0	8	0	28	0(0/28)

Note: "+" means positive; "-" means negative

Distance ratio = (percentage of pathogenicity above 50% − 50%) / (percentage of pathogenicity above 50% - percentage of pathogenicity below 50%) = (75% − 50%) / (75% − 18.75%) = 0.44, lgTCID50 = distance ratio × difference between logarithms of dilution + logarithm of dilution with pathogenicity above 50%=0.44×(-1)+(-6) = 6.44 and TCID50 = $10^{-6.44}$/0.1 ml

infected cells reacted with the fluorescent antibody, exhibiting green fluorescence (Fig. 4).

Transmission electron microscopy observation

Negative stained BKV particles exhibited a spherical morphology with a diameter of approximately 20–30 nm (Fig. 5).

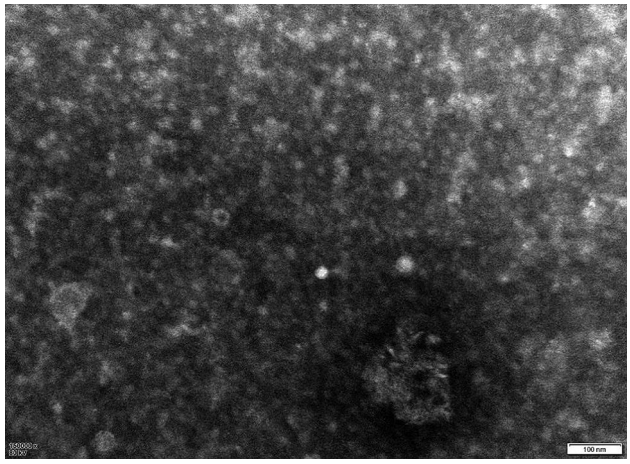

Fig. 5 Photos of the TEM images (150000×)

Genome amplification and sequencing

The 11 pairs of designed BKV whole genome-specific amplification primers were used to perform PCR amplification on the BKV cell samples identified as positive. The RT-PCR amplification products were subjected to 1% agarose gel electrophoresis and visualized using a gel documentation system. The target bands of 756 bp, 721 bp, 1306 bp, 832 bp, 1047 bp, 1219 bp, 1208 bp, 498 bp, 975 bp, 1032 bp, and 819 bp were obtained, matching expected size (Fig. 6). The specific bands that met the expected size were excised and recovered, and the plasmids extracted after T-A cloning were sent to Shanghai Sangong Biological Engineering Co., Ltd.

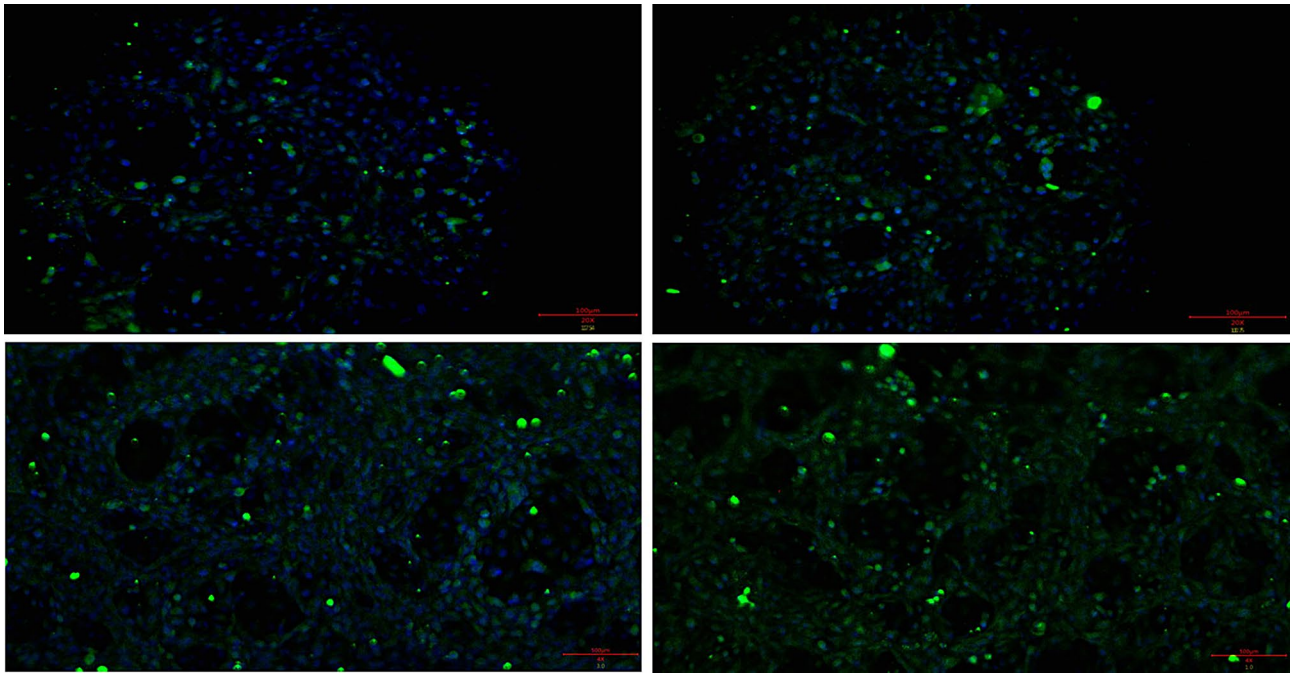

Fig. 4 IFA identification of Vero cells infected with BKV

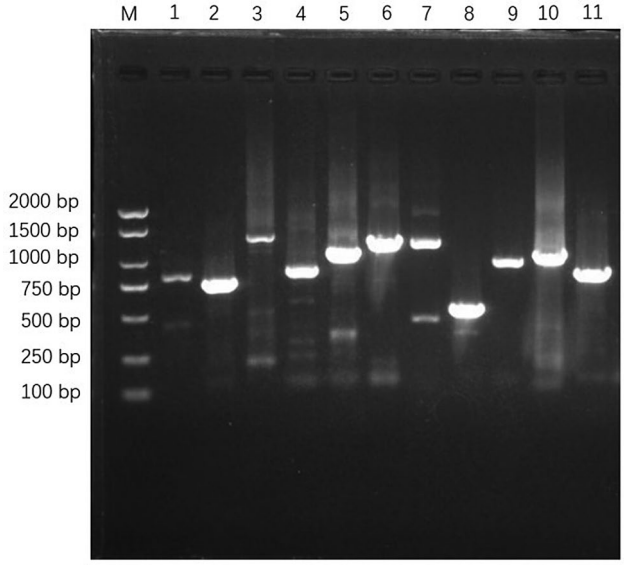

Fig. 6 PCR amplification results of the whole genome of BKV YN-1. M: DL2000 marker; 1–11: Various fragments amplified from the BKV YN-1 genome

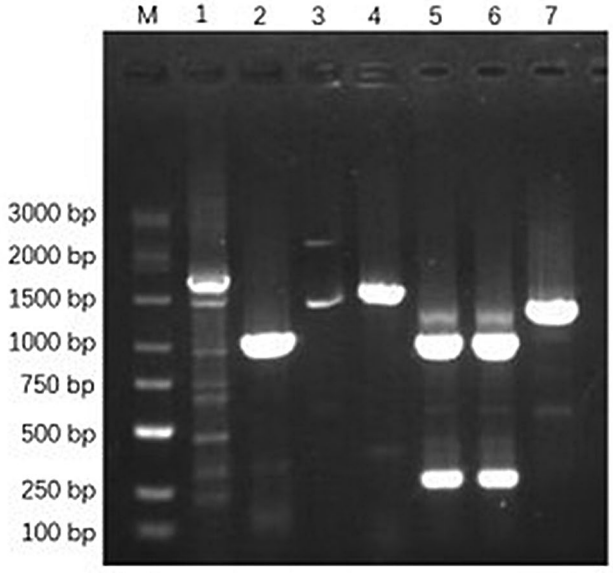

Fig. 7 PCR amplification results of the whole genome of BKV YN-2. M: DL3000 marker; 1–7: Various fragments amplified from the BKV YN-2 genome

(Kunming Branch)for sequencing. The sequencing results were consistent with expectations, and the BKV YN-1 whole genome was successfully amplified.

The BKV-positive viral sample was PCR amplified using 7 pairs of BKV genome-specific primers. The RT-PCR products were analyzed using 1% agarose gel electrophoresis and visualized using a gel documentation system. Specific bands of 1500 bp, 1008 bp, 1419 bp, 1594 bp, 1013 bp, 1173 bp, and 1313 bp were obtained, matching the expected sizes (Fig. 7). The bands of the expected size were excised, gel-purified, and cloned into a T-vector. After plasmid extraction, Shanghai Sangong Biological Engineering Co., Ltd. (Kunming Branch) performed sequencing. The sequencing results aligned with the expected sequences, and the full genome of BKV YN-2 was successfully amplified.

Genomic characteristics of BKV

Genomic structure features

The sequencing results of RT-PCR-positive recombinant plasmids were assembled and analyzed using the SeqMan software in DNASTAR. The assembled sequences were compared with the published Bovine BKV U-1 strain target fragment sequences available in NCBI and GenBank databases using SnapGene 6.02 software to confirm the identity of the BKV genomic fragments. The two assembled sequences were designated as BKV YN-1 2023 and BKV YN-2 2023, with genome lengths of 8289 bp and 8291 bp, respectively (GenBank No. PV410179 and PV410180).

The BKV genomes comprised typical structural and non-structural regions, including the 5'-UTR, L, VP0, VP3, VP1, 2 A, 2B, 2 C, 3 A, 3B, 3 C, 3D, and 3'-UTR, as illustrated in Fig. 8. Both genomes exhibited a GC content of 55% and retained the standard BKV genomic organization. Specifically, BKV YN-1 contained a complete 7398 bp ORF, while BKV YN-2 harbored a slightly longer 7395 bp ORF. The open reading frames (ORFs) encoded a polyprotein composed of the leader protein (L), structural proteins (P1: VP0, VP3, and VP1), and non-structural proteins (P2: 2 A, 2B, and 2 C; P3: 3 A, 3B, 3 C, and 3D). These results confirm that the two BKV genomes exhibit the standard genomic organization and conserved structural features characteristic of BKV. The structure of the two isolates and the location and size of each gene are shown in Fig. 8; Table 2.

Phylogenetic analysis

The complete genomes of BKV YN-1 2023 and BKV YN-2 2023 were analyzed alongside 40 reference sequences representing genotypes A–F from GenBank using MAGE 7.0 software to construct a phylogenetic tree. In the phylogenetic trees based on the complete genomes, these strains were grouped into the BKV-B species (Fig. 9). P1 structural protein is the main component of the viral capsid, which contains structural subunits such as VP0, VP1, and VP3. These subunits are directly involved in the binding process between the virus and the host cell receptor [15]. The analysis of the P1 protein region is crucial for understanding the molecular evolution of the virus. To further investigate the molecular characteristics of the P1 region in BKV YN-1 2023 and BKV YN-2 2023, this study selected P1 region sequences from other kobuviruses available in GenBank for phylogenetic analysis (Fig. 10).

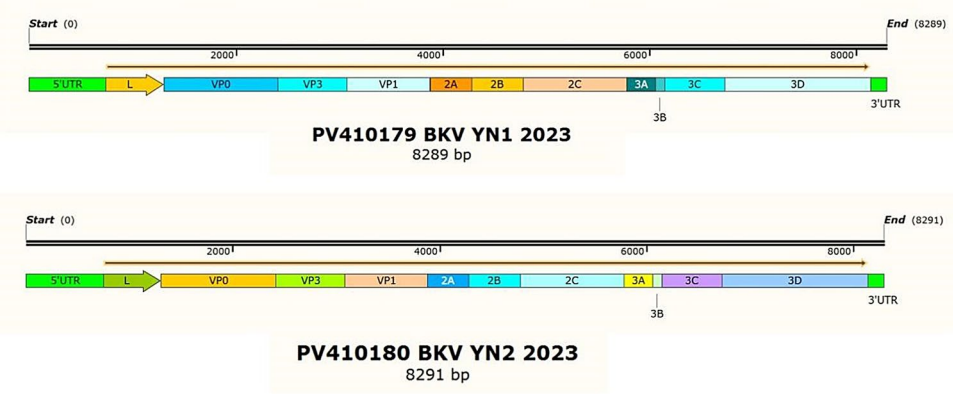

Fig. 8 Genome characteristics of BKV YN-1 2023 and BKV YN-2 2023

Table 2 The location and size information of each gene of the two isolates

Gene		BKV YN-1 2023			BKV YN-2 2023		
		Location	Size /bp	GC%	Location	Size	GC%
5'UTR		1 ~ 746	746	52%	1 ~ 746	751	52%
L		747 ~ 1 307	561	55%	752 ~ 1 312	561	55%
P1	VP0	1 308 ~ 2 411	1 104	59%	1 313 ~ 2 416	1104	59%
	VP3	2 412 ~ 3 080	669	57%	2 417 ~ 3 085	669	56%
	VP1	3 081 ~ 3 881	801	57%	3 086 ~ 3 886	801	56%
P2	2 A	3 885 ~ 4 286	402	57%	3 887 ~ 4 288	402	57%
	2B	4 287 ~ 4 781	495	55%	4 289 ~ 4 783	495	54%
	2 C	4 782 ~ 5 786	1 005	56%	4 784 ~ 5 788	1005	57%
P3	3 A	5 787 ~ 6 068	282	55%	5 789 ~ 6 070	282	55%
	3B	6 069 ~ 6 158	90	61%	6 071 ~ 6 160	90	62%
	3 C	6 159 ~ 6 734	576	54%	6 161 ~ 6 736	576	54%
	3D	6 735 ~ 8 144	1 410	53%	6 737 ~ 8 146	1410	53%
3'UTR		8 145 ~ 8 289	145	57%	8 147 ~ 8 291	145	53%

The results revealed the following: The P1 region sequences of BKV YN-1 2023 and BKV YN-2 2023 clustered within the Bovine kobuvirus B genotype (BKV-B) group but formed a distinct branch. The genetic distance between the two strains was relatively close. This finding aligns with the phylogenetic tree constructed based on whole-genome sequences, further supporting the genetic continuity of these strains. The VP1 protein of BKV is exposed on the surface of viral particles, subjecting it to significant environmental pressures. Due to strong immune selection pressure, VP1—the most immunodominant protein in BKV—exhibits a high mutation rate. VP1 is critical in the virus's pathogenic mechanisms and receptor recognition processes, highlighting its importance in viral evolution and host adaptation [16]. To further elucidate the evolutionary relationships among BKV YN-1 2023, BKV YN-2 2023, and other BKV-B strains, this study analyzed the VP1 gene sequences from 23 BKV strains isolated from different hosts. The phylogenetic tree, constructed using the Neighbor-Joining method (Fig. 11), revealed distinct evolutionary branches among VP1 genes from different hosts. This indicates a degree of conservation in the VP1 gene across host species. Both isolates in this study clustered within the 2021 Chinese BKV branch derived from cattle but showed some evolutionary divergence. Notably, BKV YN-1 2023 had the closest genetic distance to the BKV HB-SJZ strain, and BKV YN-2 2023 had the closest genetic distance to the BKV13 strain, forming an independent sub-branch, suggesting genetic diversity among BKV strains circulating in Yunnan Province. MEGA software was used to compare and visualize the amino acid distribution of the VP1 protein among different BKV strains isolated from cattle (Fig. 12). This analysis effectively highlights amino acid variations. Notably, the R^{82} residue in the BKV YN-1 2023 isolate differs from that of other strains, while the M amino acid at position M^{196} in the BKV YN-2 2023 isolate also shows a distinct variation compared to the others.

In summary, the consistent clustering of BKV YN-1 2023 and BKV YN-2 2023 with other BKV-B strains, alongside their distinct sub-branching, suggests both regional adaptation and potential genetic diversification. Future studies incorporating additional isolates from neighboring regions will be essential for further

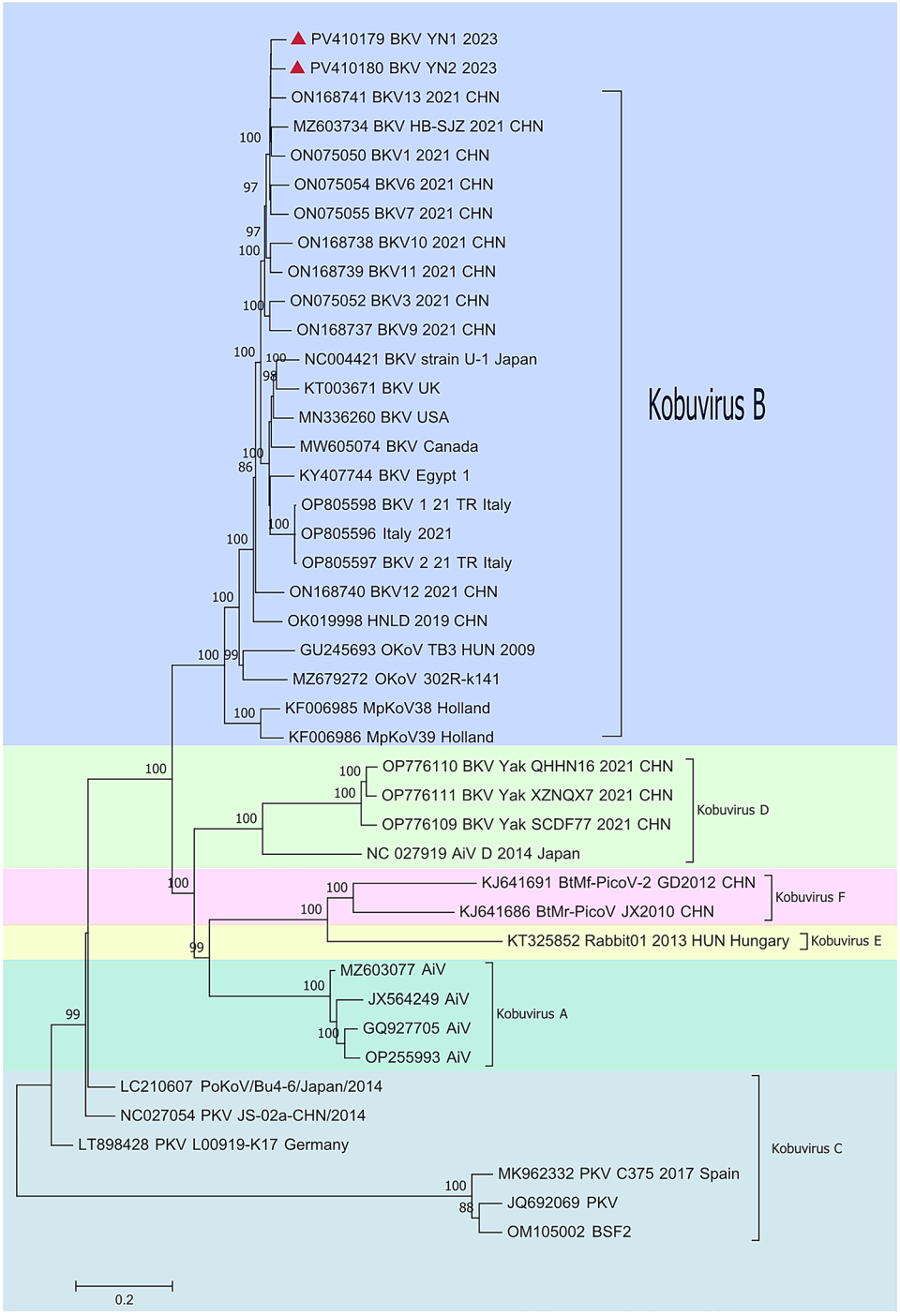

Fig. 9 Phylogenetic tree of the genomes of six species (A to F) of BKV. The Neighbor-Joining method in combination with 1,000 bootstrap replicates was used to derive a phylogenetic tree based on the complete genome sequences of six BKV strains. Red triangles (▲) represent the BKV strains from this study

elucidating the transmission pathways and evolutionary trajectory of BKV-B.

Genomic similarity analysis

The genetic similarity of the two BKV isolates identified in this study was assessed by comparing their nucleotide and amino acid sequences with those of other genotypes (Table 3). Genome-wide nucleotide sequence analysis revealed that BKV YN-1 2023 shared the highest similarity (93.7%) with BKV13 2021 CHN and the lowest similarity (39.9%) with BtMr-PicoV/JX2010. Similarly, BKV YN-2 2023 exhibited nucleotide sequence similarity

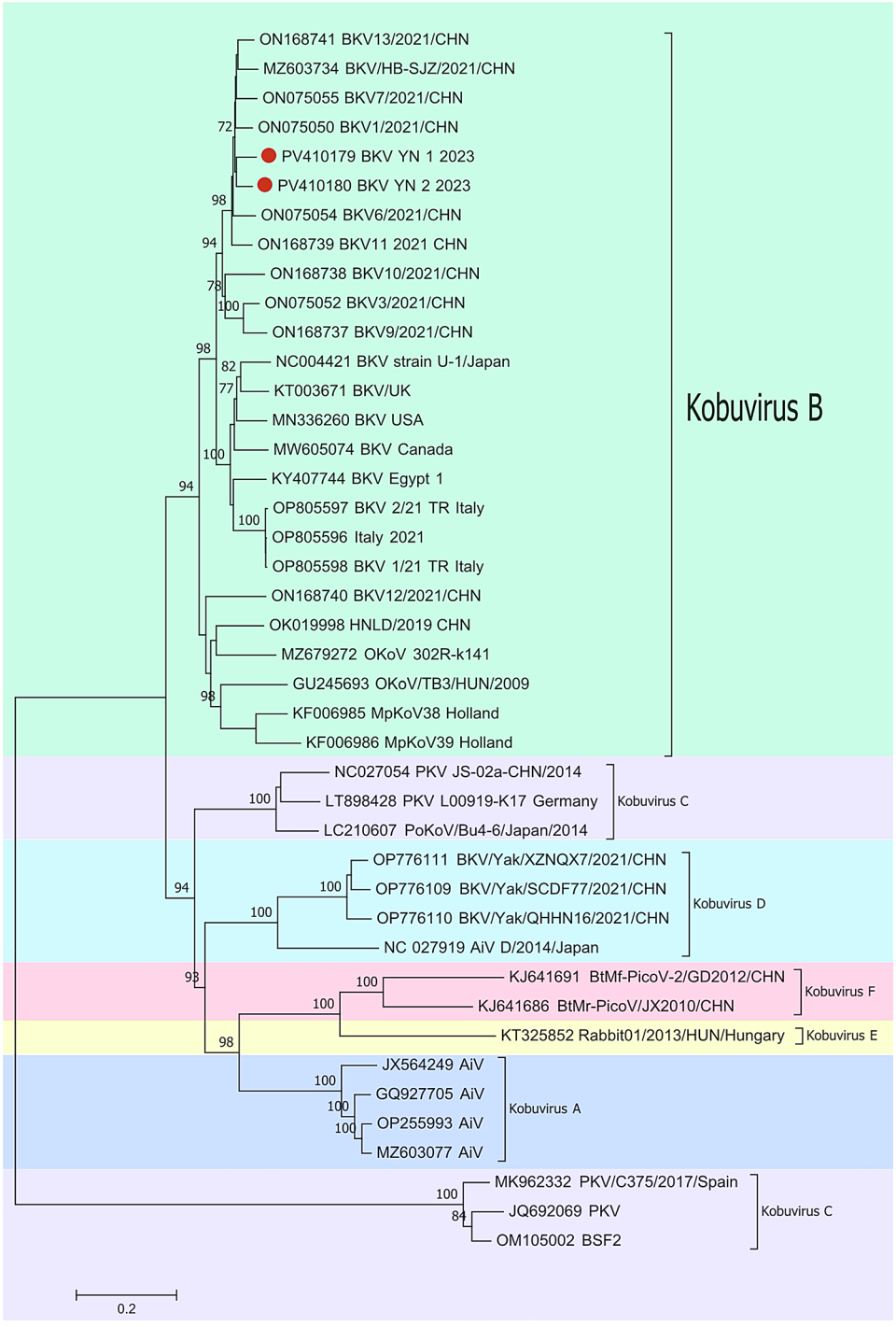

Fig. 10 Phylogenetic tree of the P1 of six species (A to F) of BKV. The Neighbor-Joining method in combination with 1,000 bootstrap replicates was used to derive a phylogenetic tree based on the complete genome sequences of six BKV strains. Red circle (●) represent the BKV strains from this study

ranging from 40.0% (BtMr-PicoV/JX2010) to 93.9% (BKV13 2021 CHN). When compared to the BKV U-1 strain, the nucleotide similarity of BKV YN-1 2023 and BKV YN-2 2023 was 79.1% and 79.3%, respectively.

At the ORF level, nucleotide sequence similarity among different BKV genotypes ranged from 48.7 to 93.9%, while amino acid sequence similarity varied from 29.3 to 98.5%. Compared to BKV13 2021 CHN, both isolates exhibited high conservation in structural proteins (VP0, VP3) and nonstructural proteins (2 A, 2B, 2 C, 3 A, 3 C, and 3D), with sequence identities ranging from 97.8 to 100%. In contrast, the L protein showed the lowest

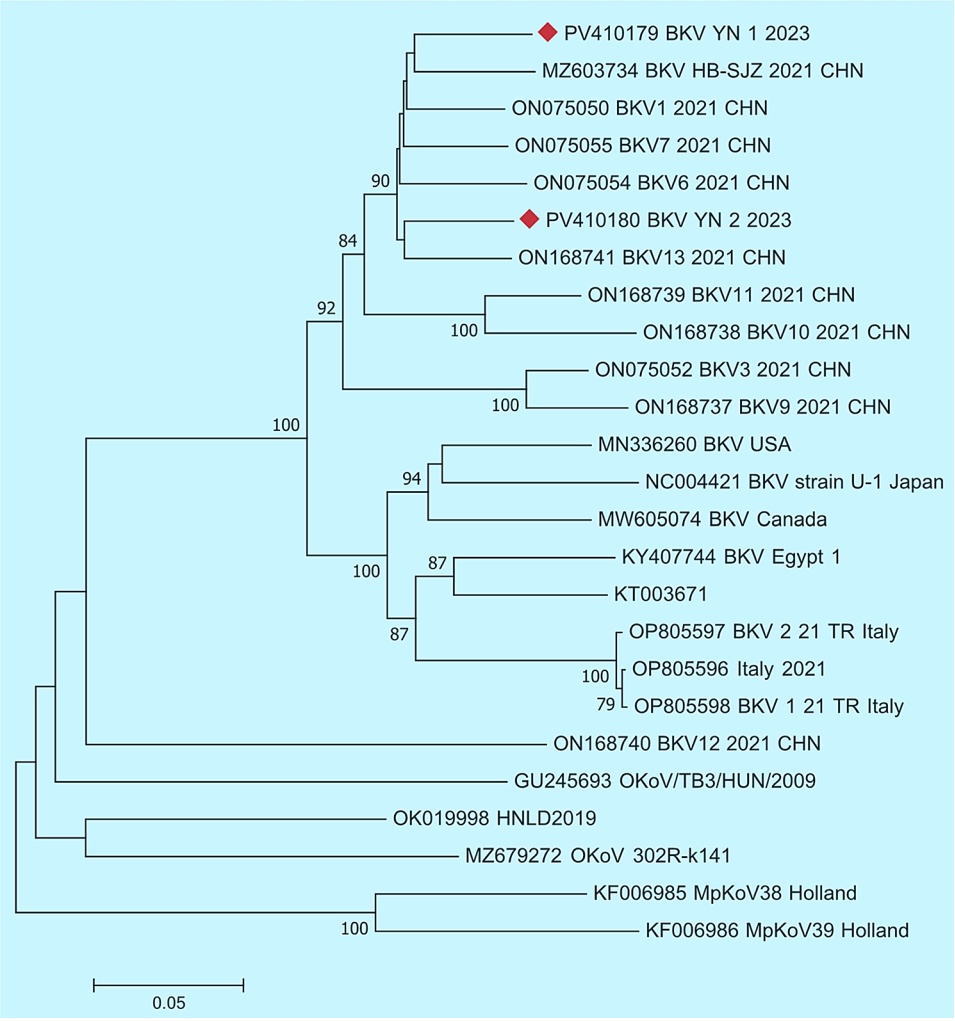

Fig. 11 Phylogenetic tree of the VP1 of the Host bovine of BKV. The Neighbor-Joining method in combination with 1,000 bootstrap replicates was used to derive a phylogenetic tree based on the complete genome sequences of six BKV strains. Red rhombus (◆) represent the BKV strains from this study

similarity, with identities of 94.7% and 95.2% for BKV YN-1 2023 and BKV YN-2 2023, respectively. Furthermore, the 5′ untranslated region (UTR) exhibited lower sequence similarity than the 3′ UTR, suggesting potential variations in regulatory elements.

Discussion

Since its first identification in Japan in 2003, BKV has demonstrated a rapid global spread and broad host tropism. To date, BKV infections have been reported in cattle, pigs, sheep, cats, dogs, mice, rabbits, ferrets, and even humans [17]. Additionally, BKV has been detected in the sewage systems of several European countries. Furthermore, detection using RT-PCR technology has shown that the overall infection rate of BKV ranges from 1 to 34.5%, with the highest prevalence observed in diarrheic cattle in South Korea [1, 18]. In this study, 204 fecal samples were collected from different cattle farms in Yunnan Province, and 40 positive samples were detected, yielding a positivity rate of 19.6%. BKV can be transmitted through both direct and indirect contact, primarily via contaminated drinking water and feces among animals. Studies have demonstrated that KoV can spread across species, such as sheep, to carnivores like ferrets, bats to rabbits, or carnivores to humans and birds [19]. In Japan, KoV transmission from pigs to cattle has also been documented [20]. Close contact between different animal species may increase the likelihood of interspecies transmission. Although KoV has been detected in many hosts, the potential for cross-species infection remains uncertain and warrants further investigation to elucidate its evolutionary relationships and host range.

The Bovine Kubovirus type B has been reported in several countries, including Thailand, South Korea, Belgium, Hungary, Netherlands, Italy, and Brazil [17, 21, 22]. The primary host of BKV-B is cattle, with reports also identifying its presence in sheep and ferrets [23]. This study systematically analyzed the whole genomes, P1 genes,

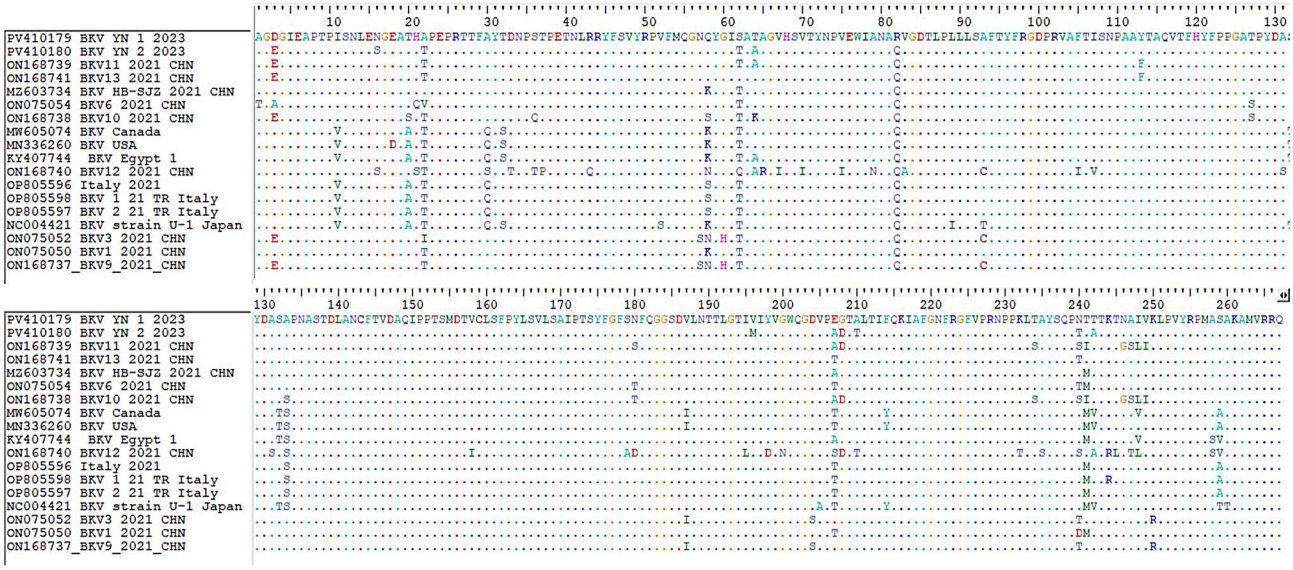

Fig. 12 Alignment of the VP1 of the Host bovine of BKV. Multiple sequence alignment was performed using MEGA 7.0 of the ClustalW algorithm

and VP1 genes of two BKV-B strains isolated from Yunnan Province, China (BKV YN-1 2023 and BKV YN-2 2023), to uncover their molecular characteristics and genetic evolutionary relationships.

Phylogenetic analysis of the whole genome revealed that both strains clustered within the same branch as reference BKV-B strains and shared the closest genetic distance with the Chinese strain BKV13 isolated in 2021. This finding indicates genetic continuity and regional transmission patterns of BKV-B in Yunnan. Further analysis of the P1 gene showed that these strains exhibited closer genetic relationships with strains isolated from cattle and sheep hosts, suggesting that cattle and sheep may play key roles in the viral transmission pathways. This highlights the adaptive evolutionary mechanisms of BKV-B in cross-host transmission.

The successful isolation of BKV remains a challenge due to the limited availability of stable cell lines suitable for viral propagation. In this study, BKV was effectively isolated from fecal samples of diarrheic calves using Vero cells. After three blind passages, significant CPE was observed, and the viral load progressively increased with successive passages. Following multiple passages, stable CPE was consistently detected. Electron microscopy of negatively stained viral supernatants revealed spherical viral particles approximately 30 nm in diameter, consistent with the known morphology of BKV virions. These findings provide a fundamental basis for further investigations into BKV pathogenesis.

The primary objective of this study was to assess the adaptability of BKV in Vero cells and to monitor viral load dynamics over successive passages. To ensure that viral replication characteristics were accurately represented, we designated passage 11 as the experimental endpoint. This approach minimized potential confounding factors associated with prolonged culture, such as adaptation-induced genetic changes or cellular exhaustion, which could influence viral behavior and growth patterns.

By passage 11, a decline in Vero cell proliferation was observed, accompanied by pronounced CPE, including cell rounding, fusion, and detachment in some wells. Since compromised cell viability can impact stable viral amplification, further passaging was discontinued to maintain the reliability and reproducibility of the findings. Additionally, genetic stability is a critical factor in long-term viral propagation. Previous studies have indicated that extended passaging may introduce mutations or recombination events, potentially altering viral biological properties [24]. While our study did not assess genomic changes beyond passage 11, future research should incorporate whole-genome sequencing of passaged viruses to evaluate genetic stability and potential adaptive mutations over extended culture periods.

Resource constraints also influenced the experimental design. Given the limited timeframe and available resources, we prioritized key experiments and data analysis within a feasible study period. At passage 11, the viral load had reached a high level, and the virus exhibited strong replication capacity, supporting the decision to conclude passaging at this stage. Future investigations should explore extended passaging, develop alternative culture systems like bovine intestinal organoid models to recapitulate in vivo infection dynamics, and investigate BKV interactions with co-infecting enteropathogens. These efforts will advance vaccine design and targeted control strategies against this emerging pathogen.

Table 3 BKV YN-1 2023 and BKV YN-2 2023 Nt and Aa identity with other kobuvirus genome sequences

	Shared nt identity (%)/aa identity (%)							
Gene region	**The BKV strains from this study**	**Kobuvirus-A**	**Kobuvirus-B**	**Kobuvirus-B**	**Kobuvirus-C**	**Kobuvirus-D**	**Kobuvirus-E**	**Kobuvirus-F**
		Homo sapiens /kvgh99012632/2010	**Bovine/U-1**	**Cow/BKV13 2021 CHN**	**Porcine/JS-02a-CHN/2014/China**	**Yak/ BKV/Yak/SCDF77/2021/CHN**	**Rabbit/ Rabbit01/2013/HUN**	**Myotis ricketti/ BtMr-PicoV/ JX2010**
5'UTR	YN1	31.5	73.8	77.8	20.7	37.5	28.7	-
	YN2	31.4	73.3	78.7	20.6	37.5	28.8	-
L	YN1	39.3/**18.9**	83.1/**66.7**	93.8/**95.2**	36.7/**15.4**	36.0/**15.9**	37.9/**16.4**	40.5/**19.9**
	YN2	39.5/**18.4**	82.5/**66.7**	94.5/**94.7**	36.4/**13.9**	35.4/**13.9**	37.4/**13.4**	39.3/**18.4**
VP0	YN1	62.6/**48.5**	84.7/**77.4**	91.4/**98.1**	68.0/**57.4**	59.6/**45.2**	47.7/**27.7**	52.3/**33.8**
	YN2	62.5/**48.2**	84.4/**76.9**	93.5/**98.4**	69.0/**57.4**	60.1/**45.2**	48.3/**29.2**	51.8/**33.2**
VP3	YN1	63.2/**57.4**	82.7/**94.2**	93.9/**97.8**	65.3/**62.8**	63.7/**61.0**	56.5/**56.1**	57.2/**56.5**
	YN2	62.9/**57.8**	82.1/**94.2**	94.9/**98.2**	66.2/**63.2**	63.8/**61.9**	56.1/**57.0**	57.1/**57.4**
VP1	YN1	45.7/**28.7**	84.9/**92.1**	92.2/**96.6**	59.0/**52.8**	52.0/**42.6**	42.0/**25.9**	38.4/**22.2**
	YN2	44.1/**27.8**	84.3/**91.2**	93.2/**96.6**	59.1/**53.2**	52.2/**42.1**	41.2/**26.4**	37.8/**22.2**
2 A	YN1	68.1/**65.0**	93.2/**96.7**	91.0/**98.5**	73.2/**73.3**	43.4/**36.7**	46.5/**45.6**	49.1/**48.3**
	YN2	68.3/**66.1**	93.0/**95.0**	93.0/**98.5**	74.0/**74.4**	44.1/**38.3**	47.2/**45.6**	48.9/**48.9**
2B	YN1	67.3/**59.1**	89.7/**86.4**	93.9/**99.4**	52.3/**67.7**	39.0/**26.4**	53.3/**43.6**	50.7/**39.1**
	YN2	67.8/**60.0**	88.8/**85.9**	93.1/**98.8**	51.9/**68.6**	38.9/**25.9**	53.4/**44.1**	50.7/**40.0**
2 C	YN1	68.4/**44.7**	89.3/**74.9**	93.8/**99.4**	72.3/**49.0**	60.6/**34.0**	54.1/**27.7**	54.5/**26.8**
	YN2	67.9/**43.8**	89.1/**72.6**	92.0/**99.4**	71.8/**47.8**	61.2/**33.4**	53.0/**26.8**	54.8/**28.2**
3 A	YN1	34.5/**18.9**	88.9/**72.6**	94.8/**100**	35.5/**14.7**	35.2/**16.8**	34.1/**17.9**	36.9/**16.8**
	YN2	34.1/**15.8**	88.9/**72.6**	95.3/**99.5**	35.2/**13.7**	33.8/**13.7**	33.4/**16.8**	37.6/**18.9**
3B	YN1	44.6/**16.7**	95.7/**90.0**	95.6/**96.7**	40.2/**10.0**	37.0/**10.0**	42.4/**10.0**	40.2/**16.7**
	YN2	45.7/**20.0**	96.7/**93.3**	95.6/**96.7**	38.0/**10.0**	38.0/**13.3**	43.5/**13.3**	40.2/**16.7**
3 C	YN1	57.0/**23.7**	93.1/**83.3**	94.8/**100**	65.2/**39.4**	51.4/**20.7**	43.4/**15.7**	44.5/**15.2**
	YN2	57.1/**25.3**	93.8/**85.9**	95.3/**99.5**	65.7/**40.4**	51.9/**19.7**	43.2/**15.7**	44.0/**14.6**
3D	YN1	70.8/**49.4**	92.3/**83.8**	95.0/**99.6**	74.1/**56.7**	65.4/**44.3**	61.0/**39.9**	61.1/39.3
	YN2	71.0/**49.8**	92.2/**84.2**	94.5/**99.4**	73.5/**54.4**	64.7/**43.5**	61.1/**41.4**	61.2/**39.3**
3'UTR	YN1	27.2	78.8	87.8	64.5	50.2	54.1	17.0
	YN2	27.6	78.4	83.8	67.1	51.9	54.1	17.7
Compleete	YN1	51.4	79.3	93.7	59.9	50.3	41.3	39.9
	YN2	51.1	79.1	93.9	60.0	50.5	41.3	40.0
ORF	YN1	61.2/**43.2**	88.2/**76.3**	93.6/**98.5**	66.9/**47.4**	57.0/**37.8**	48.8/**29.3**	50.9/**30.0**
	YN2	61.0/**43.0**	88.1/**75.7**	93.9/**98.4**	67.0/**47.6**	57.0/**37.8**	48.7/**29.3**	50.8/**30.3**

Notes: nt: Nucleotide; aa: Amino acid; BKV: Bovine kobuvirus; UTR, Untranslated region; ORF, Open reading frame. aa identity shown in bold

YN1:BKV YN-1 2023; YN2:BKV YN-2 2023

Conclusion

In conclusion, a 19.6% prevalence rate was found in diarrhea calves, and two genotype B BKV strains were isolated. The findings from this study provide valuable insights into the molecular evolution of BKV-B, offering a theoretical foundation and practical guidance for vaccine development and studies on cross-host transmission mechanisms.

Methods

Study areas and samplings

A total of 204 fecal samples were collected from diarrheic calves on cattle farms in four regions of Yunnan Province: Xuanwei City ($n = 7$), Xundian County ($n = 123$), Wuding County ($n = 14$), and Weishan County ($n = 31$).

Sampling was conducted through convenience sampling during veterinary diagnostic visits between January 2023 and December 2024. Freshly excreted fecal samples were collected from the ground immediately after defecation, using sterile tubes containing PBS (pH 7.4) with 1% penicillin-streptomycin, and transported on dry ice to the laboratory for processing within 24 h.

Experimental materials

The following reagents and materials were used in the study: fetal bovine serum, DMEM culture medium, trypsin digestion solution, cell cryopreservation solution, EvoM-MLV reverse transcription premix kit, 2×EasyTaq PCR SuperMix, 2× Apex HF FS PCR Master Mix, universal virus concentration reagent, SYBR Green Pro Taq HS qPCR premix kit, universal tissue fixation solution, FITC-conjugated AffiniPure Goat Anti-Mouse IgG (H + L), and DAPI antifade mounting medium. All reagents were purchased from Vazyme Biotech Co., Ltd.

0.2 ml Thin Wall PCR Tubes (Clear, Flat Caps, Axygen), BeyoGold™ qPCR Strip Tubes, 0.2 ml, 8 Tubes/strip, Flat Strip Caps, Clear, BeyoGold™ 25 cm^2 Cell Culture Flasks with Vented Cap, and Disposal Syringe for Experiment(Sterile independent packaging, With needle,5 ml) All consumables were purchased from Beyotime Biotechnology Co., Ltd.

The Vero cell line used in this study was preserved in our laboratory.

BKV culture

Approximately 1 g of fecal sample was mixed with 2 mL of PBS containing 1% penicillin-streptomycin and placed on a vortex shaker for 30 s. The mixture was then incubated at 4 °C overnight for proper mixing and viral extraction. After incubation, the sample was centrifuged at 12,000 rpm for 15 min at 4 °C to remove debris, leaving the supernatant containing the virus. The supernatant was then passed through a 0.22 μm sterile disposable filter to remove any remaining particulate matter, ensuring a clean viral solution for subsequent use. The BKV-positive viral supernatant was filtered using a BeyoGold™ Syringe Filter (0.22 μm/33 mm, PES, Sterile). Two flasks of healthy Vero cells were selected, and when the cells reached approximately 80% confluence, they were rinsed three times with filtered PBS. A total of 1 mL of the filtered viral supernatant was added to each flask to infect the cells, followed by incubation for 2 h in a cell culture incubator, with gentle shaking every 20 min to facilitate viral adsorption. After removing the viral supernatant, 5 mL of serum-free culture medium was added to each flask, and the cells were cultured for three days. The flasks were sealed with parafilm and subjected to three cycles of freeze-thawing at − 80 °C to release the virus. The culture medium was filtered again with a BeyoGold™ Syringe Filter (0.22 μm/33 mm, PES, Sterile) to remove cell debris. The filtered supernatant was used to inoculate fresh Vero cells. After three blind passages, the viral supernatant was subjected to RT-PCR using BKV-specific primers. If the result was positive, further passages were performed.

RT-PCR detection

To release viral RNA, filtered cell culture supernatants were subjected to three freeze-thaw cycles at − 80 °C. Total RNA was extracted using TRIzol® Reagent (Takara Bio Inc., Japan; Cat. No. 9108) and reverse transcribed into cDNA using the EvoM-MLV reverse transcription premix kit (Vazyme Biotech Co., Ltd.), following the respective manufacturer's instructions. RT-PCR was carried out using primers specific to the BKV 3D gene (BKV 3D-F: CATGCTCCTCGGTGGTCTCA; BKV 3D-R: GTCCGGGTCCATCACAGGGT; expected product size: 631 bp), with amplification performed using the 2× EasyTaq PCR SuperMix. PCR products were analyzed using agarose gel electrophoresis to confirm the presence of BKV infection.

Quantitative real-time PCR (qPCR)

Virus supernatants from the 3rd, 5th, 7th, 9th, 10th, and 11th passages were subjected to three freeze-thaw cycles, centrifuged at 12,000 rpm for 15 min at 4 °C, and the supernatants were collected. Total RNA was extracted using TRIzol® Reagent and reverse transcribed into cDNA as described above. qPCR was performed using primers designed in the conserved region of the BKV 3D gene (BKV SYBR-qF: CGAAGATTATCTCGTGAAA; BKV SYBR-qR: GCTGACAGGACACAGATG), selected to avoid primer dimerization, mismatches, or non-specific amplification. To measure viral genome copy numbers from different passage levels, quantitative real-time PCR (qPCR) was performed using the StepOnePlus™ Real-Time PCR System (Applied Biosystems, USA) in a total reaction volume of 20 μL, containing 10 μL of 2× Green Pro Taq HS Premix (Rox Plus)(Vazyme Biotech

Co., Ltd), 0.4 μL each of forward and reverse primers, 2 μL of DNA template, and RNase-free water to make up the final volume. A recombinant plasmid standard was constructed and subjected to 10-fold serial dilutions ranging from 10^1 to 10^9 copies, with each dilution tested in triplicate. The qPCR cycling conditions were as follows: initial denaturation at 95 °C for 30 s, followed by 40 cycles of 95 °C for 5 s and 60 °C for 30 s. A melting curve analysis was performed at the end of the amplification to verify the specificity of the PCR products. A standard curve was generated by plotting the Ct values against the logarithm of the copy numbers of the standard plasmid, which was then used to calculate the copy number of target genes in the samples. All reactions were performed in triplicate, and data were analyzed using one-way analysis of variance (ANOVA) with GraphPad Prism version 9.0.0 (121).

TCID50 assay

Healthy Vero cells were digested with trypsin, resuspended in DMEM containing 10% FBS, and seeded into 96-well plates. After reaching approximately 85% confluence, the viral supernatants were serially diluted in DMEM with 10% FBS (10-fold dilutions across 10 gradients). The medium was removed from the 96-well plates, and 100 μL of each dilution was added to eight wells per dilution. The plates were incubated at 37 °C with 5% CO_2 for 2 h to allow viral adsorption, then the supernatants were removed, and 100 μL of serum-free maintenance medium was added to each well. The plates were incubated for three days, and cytopathic effects (CPE) were observed under an inverted microscope. Wells showing CPE were marked as "+," and those without were marked as "–." The percentage of wells with CPE was calculated for each dilution, and the $TCID_{50}$ was determined using the Reed-Muench method [14].

Indirect Immunofluorescence assay (IFA)

Healthy Vero cells were digested, resuspended in DMEM containing 10% FBS, and seeded into 6-well plates. After cells reached confluence, viral supernatant was added. At 36 h post-infection, the cells were washed three times with PBS (2 min each), fixed with 4% paraformaldehyde for 15 min, and permeabilized with 0.5% Triton X-100 for 15 min at room temperature. After washing with PBS, cells were blocked with 10% BSA for 2 h. Primary mouse anti-BKV antibody (dilution 1:200) was added and incubated overnight at 4 °C. After washing with PBST (PBS containing 0.05% Tween-20), a fluorescent secondary antibody (rabbit anti-mouse IgG, dilution 1:200) was added and incubated at 37 °C for 1 h. The cells were washed again with PBS and observed under a fluorescence microscope.

Electron microscopy of viral particles

After Vero cells were infected with BKV, the viral supernatant was collected, freeze-thawed three times, and centrifuged at 12,000 rpm for 10 min to remove cell debris. The supernatant was further centrifuged at 40,000 rpm for 5 h using an ultracentrifuge, resulting in a white, cloudy precipitate at the tube bottom. The supernatant was discarded, and the pellet was resuspended in 20 μL of viral preservation solution. The sample was transferred to a 1.5 mL tube and sent to Chengdu Lilai Biotechnology Co., Ltd. for transmission electron microscopy.

Genome amplification and sequencing

Published BKV sequences available in GenBank were aligned using MEGA 7.0 for multiple sequence alignment. Primer pairs were designed with default parameters using Primer Premier 5.0 (PREMIER Biosoft, USA) and synthesized by Shanghai Sangong Biological Engineering Co., Ltd. (Kunming Branch) (Table 4). Total RNA was extracted from BKV viral suspensions using TRIzol® Reagent (Takara Bio Inc., Japan; Cat. No. 9108) and reverse transcribed into cDNA using the EvoM-MLV reverse transcription premix kit, according to the manufacturer's instructions.

PCR amplification was conducted using the synthesized cDNA as a template. For full-genome amplification of isolates, 2× Apex HF FS PCR Master Mix (Vazyme Biotech Co., Ltd) was employed to ensure high-fidelity amplification suitable for sequencing and downstream genetic analysis. PCR products were analyzed by electrophoresis on a 1.5% agarose gel. Bands corresponding to the target genes were excised, and DNA was purified from the gel. The purified products were then ligated into the pMD19-T vector for T-A cloning to obtain recombinant plasmids. Positive recombinant clones were sent to Shanghai Sangong Biological Engineering Co., Ltd. (Kunming Branch) for Sanger sequencing.

Sequence assembly and phylogenetic analysis

The sequencing data were assembled using SeqMan software, with the BKV U-1 strain as the reference template. Gene annotation of the assembled sequences was performed using SnapGene 6.0.2 (https://www.snapgene.com). Sequence similarity analysis was conducted using the ClustalW algorithm in the Megalign module of DNASTAR [25, 26]. A phylogenetic tree based on nucleotide sequences was constructed in MEGA 7.0 using the Neighbor-Joining method and the Kimura

Table 4 BKV YN-1 whole genome amplification primers

Names	Sequences (5′-3′)	Temperature/℃	Length
BKV 5, UTR F	GCGTGCTTCGCGTCGTCGTAAGT	58℃	756 bp
BKV 5, UTR R	AGCACGGTGGGAGATGG		
BKV L F	ACTGCCATTCTCAAGTGTTC	53℃	721 bp
BKV L R	ATTCACAGTAGGGGACCAG		
BKV VP0 F	GAAACCCACTGGTAACA	51℃	1306 bp
BKV VP0 R	GCTGAACTGGTCTGCC		
BKV VP3 F	CCTCCACCAACCAGTC	50℃	832 bp
BKV VP3 R	CGAGGCTCAGGAGTATG		
BKV VP1 F	CTCCATCAGCCATCATCC	52℃	1047 bp
BKV VP1 R	ATGCCACAACAGCAGACA		
BKV 2AB F	CCGCCCTCACCATCTT	54℃	1219 bp
BKV 2AB R	TGGGAGTCGGCAAGAAT		
BKV 2 C F	ATCTGTGCGGACTTGGC	56℃	1208 bp
BKV 2 C R	ACCTCGTCGGCGTCTAT		
BKV 3AB F	TCTCATCAAGAGGCAAGG	51℃	498 bp
BKV 3AB R	ATGCGGTTGTAGAGGTAAA		
BKV 3 C-D F	CTCTTCGCCACTACCACC	54℃	975 bp
BKV 3 C-D R	CTTGTCCATGTCTCCCTTG		
BKV 3D F	GTCTCGAGCCTGGAACCAAA	58℃	1032 bp
BKV 3D R	GACGCTGGTCATCTGGAACA		
BKV3D-3,UTR F	TCGTGAAACTGACTGGT	50℃	819 bp
BKV3D-3,UTR R	GCAAGAAAAGAATAGAAAT		

two-parameter model. Bootstrap analysis was performed with 1,000 replicates to assess tree reliability [27, 28]. The final phylogenetic tree was highlighted and refined using Adobe Illustrator 2023. For VP1 analysis, multiple sequence alignments were performed in MEGA 7.0 using the ClustalW algorithm [28]. The aligned sequences were translated into amino acids and further visualized using BioEdit 7.0.9.0 [29]. The reference strain information is shown in Table 5.

Table 5 BKV reference sequence information

Genotype	Infecting the host	GenBook NO.	Country
A	Homo sapiens	JX564249	China
A	Homo sapiens	GQ927705	Germany
A	Homo sapiens	OP255993	Netherlands
A	Homo sapiens	MZ603077	Belgium
B	Cow	ON168741	China
B	Cattle	MZ603734	China
B	Cow	ON075050	China
B	Cow	ON075054	China
B	Cow	ON075055	China
B	Cow	ON168738	China
B	Cow	ON168739	China
B	Cow	ON075052	China
B	Cow	ON168737	China
B	Bovine	NC004421	Japan
B	Cattle	KT003671	Britain
B	Cattle	MN336260	America
B	Cattle	MW605074	Canada
B	Cattle	KY407744	Egypt
B	Bovine	OP805598	Italy
B	Calf	OP805596	Italy
B	Bovine	OP805597	Italy
B	Cow	ON168740	China
B	Cattle	OK019998	China
B	Domestic sheep	GU245693	Hungary
B	Sheep	MZ679272	China
B	Mustela putorius furo	KF006985	Netherlands
B	Mustela putorius furo	KF006986	Netherlands
C	Porcine	NC027054	China
C	Porcine	LT898428	Germany
C	Porcine	LC210607	Japan
C	Porcine	MK962332	Spain
C	Porcine	JQ692069	China
C	Porcine	OM105002	South Africa
D	Bos taurus	NC027919	Japan
D	Yak	OP776109	China
D	Yak	OP776110	China
D	Yak	OP776111	China
E	Rabbit	KT325852	Hungary
F	Myotis ricketti	KJ641686	China
F	Myotis ricketti	KJ641691	China

Abbreviations

KoV	Kobuviruses
BKV	Bovine Kobuvirus
AiV-D	D-type bovine kobuvirus
RT-PCR	Reverse transcription polymerase chain reaction
CPE	Cytopathic effects
qPCR	Quantitative polymerase chain reaction
ORF	Open reading frame
UTR	Untranslated region

Supplementary Information

The online version contains supplementary material available at https://doi.org/10.1186/s12917-025-04811-y.

Supplementary Material 1

Acknowledgements

We would like to express our sincere gratitude to the Yunnan Joint International R&D Center of Veterinary Public Health for their financial support under Grant [202403AP140033], and to the Manglong Rural Revitalization & Technological Innovation Village in Lianghe County for their funding under Grant [202404BU090032]. We also extend our heartfelt thanks to our families for their constant support, patience, and understanding throughout this study.

Author contributions

GJW and QHD prepared the manuscript, VP and XHD revised the manuscript, QHD, XSS and PYZ isolated and identified the viruses in cell culture, QHD, GJW and YL analyzed genome sequences, WGL and ZLL designed the study. All the

authors have read and approved the final manuscript. Guojun Wang, Qiuhui Deng both contributed equally to this work.

Funding
This study was supported by Yunnan Joint International R&D Center of Veterinary Public Health (202403AP140033), Manglong Rural Revitalization & Technological innovation Village in Lianghe County(202404BU090032).

Data availability
The datasets and materials used and/or analyzed during the current study are available from the corresponding author upon reasonable request.

Declarations

Ethics approval and consent to participate
This study did not involve direct animal interventions, as only fecal samples were collected from the environment during routine farm operations. Therefore, ethics approval was not required.

Consent for publication
Not applicable.

Competing interests
The authors declare no competing interests.

Received: 3 January 2025 / Accepted: 6 May 2025
Published online: 21 May 2025

References

1. Hao L, Chen C, Bailey K, Wang L. Bovine kobuvirus—A comprehensive review. Transbound Emerg Dis. 2021;68:1886–94.
2. Yan N, Yue H, Liu Q, Wang G, Tang C, Liao M. Isolation and characteristics of a novel aichivirus D from Yak. Microbiol Spectr. 2023;11:e00099–00023.
3. Han X, Zhang W, Xue Y, Shao S. Sequence analysis reveals mosaic genome of Aichi virus. Virol J. 2011;8:1–4.
4. Chen Y-S, Chen B-C, Lin Y-S, Chang J-T, Huang T-S, Chen J-J, Chang T-H. Detection of Aichi virus with antibody targeting of conserved viral protein 1 epitope. Appl Microbiol Biotechnol. 2013;97:8529–36.
5. Sabin C, Füzik T, Škubník K, Pálková L, Lindberg AM, Plevka P. Structure of Aichi virus 1 and its empty particle: clues to kobuvirus genome release mechanism. J Virol. 2016;90:10800–10.
6. Yamashita T, Ito M, Kabashima Y, Tsuzuki H, Fujiura A, Sakae K. Isolation and characterization of a new species of kobuvirus associated with cattle. J Gen Virol. 2003;84:3069–77.
7. Wang L, Fredrickson R, Duncan M, Samuelson J, Hsiao S-H. Bovine kobuvirus in calves with diarrhea, united States. Emerg Infect Dis. 2020;26:176.
8. Zhang M, Hill JE, Alexander TW, Huang Y. The nasal Viromes of cattle on arrival at Western Canadian feedlots and their relationship to development of bovine respiratory disease. Transbound Emerg Dis. 2021;68:2209–18.
9. Di Martino B, Di Profio F, Di Felice E, Ceci C, Pistilli MG, Marsilio F. Molecular detection of bovine kobuviruses in Italy. Arch Virol. 2012;157:2393–6.
10. Mohamed FF, Mansour SM, Orabi A, El-Araby IE, Ng TFF, Mor SK, Goyal SM. Detection and genetic characterization of bovine kobuvirus from calves in Egypt. Arch Virol. 2018;163:1439–47.
11. Chang J, Wang Q, Wang F, Jiang Z, Liu Y, Yu L. Prevalence and genetic diversity of bovine kobuvirus in China. Arch Virol. 2014;159:1505–10.
12. Li Y, Liang J, Wu S, Yan Z, Zhang W. Complete genomic sequence analysis and intestinal tissue localization of a Porcine kobuvirus variant in China. Infect Genet Evol. 2022;104:105362.
13. Jeoung HY, Lim JA, Jeong W, Oem JK, An DJ. Three clusters of bovine kobuvirus isolated in Korea, 2008–2010. Virus Genes. 2011;42:402–6. https://doi.org/10.1007/s11262-011-0593-9.
14. Reed LJ, Muench H. A simple method of estimating fifty per cent endpoints. 1938.
15. Zhu L, Wang X, Ren J, Kotecha A, Walter TS, Yuan S, Yamashita T, Tuthill TJ, Fry EE, Rao Z. Structure of human Aichi virus and implications for receptor binding. Nat Microbiol. 2016;1:1–6.
16. Adzhubei AA, Sternberg MJ, Makarov AA. Polyproline-II helix in proteins: structure and function. J Mol Biol. 2013;425:2100–32.
17. Reuter G, Boros Á, Pankovics P. Kobuviruses–a comprehensive review. Rev Med Virol. 2011;21:32–41.
18. Park S-J, Kim H-K, Song D-S, Moon H-J, Park B-K. Molecular detection and genetic characterization of kobuviruses in fecal samples collected from diarrheic cattle in Korea. Infect Genet Evol. 2011;11:1178–82.
19. Lu L, Van Dung N, Ivens A, Bogaardt C, O'Toole A, Bryant JE, Carrique-Mas J, Van Cuong N, Anh PH, Rabaa MA. Genetic diversity and cross-species transmission of kobuviruses in Vietnam. *Virus evolution* 2018, *4*, vey002.
20. Khamrin P, Maneekarn N, Hidaka S, Kishikawa S, Ushijima K, Okitsu S, Ushijima H. Molecular detection of kobuvirus sequences in stool samples collected from healthy pigs in Japan. Infect Genet Evol. 2010;10:950–4.
21. Khamrin P, Maneekarn N, Peerakome S, Okitsu S, Mizuguchi M, Ushijima H. Bovine kobuviruses from cattle with diarrhea. Emerg Infect Dis. 2008;14:985.
22. Mauroy A, Scipioni A, Mathijs E, Thys C, Thiry E. Molecular detection of kobuviruses and Recombinant Noroviruses in cattle in continental Europe. Arch Virol. 2009;154:1841–5.
23. Smits SL, Raj VS, Oduber MD, Schapendonk CM, Bodewes R, Provacia L, Stittelaar KJ, Osterhaus AD, Haagmans BL. Metagenomic analysis of the ferret fecal viral flora. PLoS ONE. 2013;8:e71595.
24. Bahir I, Fromer M, Prat Y, Linial M. Viral adaptation to host: a proteome-based analysis of codon usage and amino acid preferences. Mol Syst Biol. 2009;5:311. https://doi.org/10.1038/msb.2009.71.
25. Thompson JD, Higgins DG, Gibson TJ. CLUSTAL W: improving the sensitivity of progressive multiple sequence alignment through sequence weighting, position-specific gap penalties and weight matrix choice. Nucleic Acids Res. 1994;22:4673–80.
26. Burland TG. DNASTAR's lasergene sequence analysis software. Methods Mol Biol. 2000;132:71–91. https://doi.org/10.1385/1-59259-192-2:71.
27. Hillis DM, Bull JJ. An empirical test of bootstrapping as a method for assessing confidence in phylogenetic analysis. Syst Biol. 1993;42:182–92.
28. Kumar S, Stecher G, Tamura K. MEGA7: molecular evolutionary genetics analysis version 7.0 for bigger datasets. Mol Biol Evol. 2016;33:1870–4. https://doi.org/10.1093/molbev/msw054.
29. Hall TA, BioEdit. A user-friendly biological sequence alignment editor and analysis program for Windows 95/98/NT. *Nucleic Acids Symposium Series* 1999, *41*, 95–98.

Publisher's note